

**NMR IMAGING OF FLUID SATURATION DISTRIBUTIONS IN CORES**

by

**B. A. Baldwin, Phillips Petroleum Company  
W. S. Yamanashi, Servant Institute of Radiology**

**ABSTRACT**

Applications of NMR Imaging to examine fluid distributions as a function of core treatment and the interaction between fluids and their surroundings are described. The features examined include the magnitude of heterogeneity of pore distribution, internal structure, fluid distribution after centrifuging, rate of redistribution of a wetting fluid after centrifuging, effect of pore size on image intensity and the expulsion of hydrocarbon from small pores and surfaces by water in a water-wet core. The results illustrate the potential usefulness of NMR Imaging for determining core properties.

## INTRODUCTION

Traditionally core analysts have been forced to assume that cores were homogeneous black boxes. They could measure the volumes and composition of fluids that were injected and recovered but they could only infer how the fluids were distributed inside the core. With the application of radiotracers and x-ray, gamma-ray and microwave absorption techniques it became possible to obtain one-dimensional fluid saturations along one axis as a function of time and treatment. With the advent of x-ray CAT scanning, three-dimensional rock densities and concentrations of fluids in the core could be determined (Wellington and Vinegar, 1987; Hunt et. al., 1988). Nuclear Magnetic Resonance Imaging (NMRI) measures the concentration of fluids, local environment and interactions of fluids with their surrounding (Rothwell and Vinegar, 1985; Bottomley et. al., 1987; Baldwin and Yamanashi, 1988a). This paper will describe the application of NMRI to problems of interest to reservoir scientists.

## EXPERIMENTAL

All NMR images were obtained with a Picker International MR VISTA 2005. This medical instrument had a 0.5 T superconducting magnet and operated at 21.3 MHz. The standard 1 m transmitting coil and a special 6.4 cm diameter solenoid receiving coil, which had been built to optimize signal intensity and homogeneity, were used. Fig. 1 shows the receiving coil and it's holder. The coil form (Teflon(r)) and holder (plexiglass) were not observed in the images. Hydrogen proton signals were obtained with a single spin echo Hahn sequence. The echo time, TE, was set at 26 ms and the recovery time, TR, was set at 1000 ms. Four slices, each 5 mm thick, were obtained parallel to the cylindrical axis of the core plug. This orientation produced rectangular images. The central images were used since they produced the least edge distortion from averaging over the curvature of the plug. With a 30 cm diameter field of view and 256 x 256 pixel matrix the resolution was 1.2 mm/ pixel. Under these conditions it took 8.5 minutes to obtain a set of four images across one plug.

The cores were Berea Sandstone, a chalk and a shaly sandstone. These were cleaned in methanol and toluene and saturated by evacuating to at least 100 mtorr then submerging the plug in degassed saturating fluid and returning pressure to atmospheric. The cores were 1 in. diameter and from 1 to 2 in. long. Saturating fluids were 20,000 ppm NaCl brine and heptadecane. Heptadecane was chosen as the hydrocarbon because it could be easily frozen while the core was in the centrifuge. This eliminated the possibility of redistribution of the wetting fluid prior to measurement in the NMR Imager.

## RESULTS AND DISCUSSION

Fig. 2 shows one of the central NMR images of fluid in a 100% saturated Berea core plug. A rectangular image was obtained by collecting data in a plane parallel to the long axis of the cylindrical core plug. The mottled appearance is due to variation in fluid saturation, but does not represent resolution of individual pores. An intensity profile, Fig. 3, along the major axis of this core shows variations in intensity which translate to variations in fluid saturation, but is always well above zero intensity. The white areas

represent voxels (volume elements) filled with more pore space and the dark areas voxels with less pore space. These images indicate that the heterogeneity of this Berea Sandstone is on the order of a few millimeters which can be resolved by the medical NMR Imager.

The image of a chalk plug, Fig. 4, shows two features. First the less mottled appearance indicates that the scale of heterogeneity of the pore space in this chalk plug is lower than the resolution of the medical NMR Imager. Second the drop in intensity toward the center is due to poor saturation of this plug. From the intensity profile it appears that this area is approximately 80% saturated. Although this area appears to be a rectangle it is the cross section of a cylinder with dimensional ratios the same as the outer part of the plug. This partial saturation would have gone undetected in standard gravimetric measurements because it resulted in a reduction in calculated porosity from 36.0 to 35.6 %. The low permeability of the chalk, ca. 1 md, and the shorter than normal time that this plug was in the saturation process contributed to this undersaturated central portion.

The ability to nondestructively examine the inside of a core plug could aid greatly in determining which plugs would give representative data and which plugs would contribute anomalous results due to internal structure. A comparison between NMR images and the internal structure of a plug can be made from the images in Fig. 5. The upper images are the two central NMR images of the plug saturated with brine. The lower images are photographs of the plug after slabbing along the middle of the respective image plane. The dark lines sloping upward from left to right on the left hand side of the NMR images are also observed in the photographs as brownish red lines. It appears that the low porosity is due to a filling of a burrow with cement containing iron oxide. On the right hand side of the image there are dark horizontal lines in the NMR image with no apparent corresponding feature in the cut sample. This suggests that there can be porosity/permeability variations which are not readily observed in a visual geological examination. The importance of these observations is that this sample would be a very poor plug to use for determining average reservoir matrix properties. For any type of flow measurement the barrier toward the left end would have a significant effect on the measured properties compared to a homogeneous plug. From the outside of the plug there was no indication of these features.

Another way to change local fluid saturation in a plug is to centrifuge it. This produces a saturation gradient along the centrifugal axis. Localized NMR image intensity is compared to average weight measurements for a Berea Sandstone core composed of eight discs, Fig. 6. Heptadecane was used as the saturating fluid because it could be frozen in the centrifuge and eliminate any redistribution of fluid prior to measurement. These curves were normalized, for comparison, to match at the highest saturation. There is general agreement between the two measurements, higher intensity and saturation toward the bottom of the plug. However, quantitatively there is considerable difference toward the top of the plug. Due to capillary pressure differences larger pores generally desaturate before the smaller pores. Since NMR relaxation times, and hence intensity at a given delay time, are dependent on the size of the pore (Laufer, 1981; Timur, 1969), the intensity at a lower saturation will be less than expected on a weight measurement. A calibration curve for these particular Berea Sandstone samples was determined from

equilibrium porous plate desaturation measurements and is shown in Fig. 7. The slope in this curve shows that NMR intensity decreases rapidly in the early stages of desaturation, as the larger pores are desaturated, and levels off at lower saturations as the signal approaches the noise. Due to the signal to noise limit, saturations below about 15% PV could not be determined. Using this calibration curve corrected the NMR intensity data to give good agreement between the NMRI and weight measurement data, Fig. 8, without any normalization step. Note that neither the weight or NMRI measurements showed 100 % saturation at the bottom of the plug. The slightly higher intensity with NMRI indicates that the higher resolution detected a volume with higher saturation near the bottom of the plug than the gravimetric average measured for the bottom disc.

One major concern when using the centrifuge to prepare core for additional measurements is the length of time it takes before the saturating fluids redistribute themselves to a uniform distribution. Figs. 9 to 12 show the saturation gradients of Berea Sandstone and North Sea Chalk with either heptadecane or brine. Heptadecane was used first as the saturating fluid because it could be frozen in the centrifuge until time for the NMR measurement. To maximize the saturation gradient the Berea was centrifuged at a low pressure, 1.3 psi at the top. Because of its higher capillary pressure the chalk was centrifuged at a pressure of 45 psi at the top of the plug. Images at four different times after centrifuging for each of the heptadecane saturated plugs are shown in Figs. 9 and 10. For the Berea Sandstone sample the saturation gradient in Fig. 9A was very sharp with most of the heptadecane near the bottom of the core. Eight hours later significant redistribution had occurred, Fig 9B. Note that the intensity axis is about half of the first image. At later times of 47 and 96 hrs, Fig. 9C and 9D, respectively, the saturation had moved toward a more uniform distribution. At 216 hrs the heptadecane was uniformly distributed along the Berea Sandstone plug.

Heptadecane in chalk also showed a significant saturation gradient when centrifuged, Fig. 10A. The black areas in the left-hand side of the image are electronically clipped because of the strong intensity. Some redistribution did occur as seen by the changing saturation gradient in Fig. 10B to D, but even after 330 days (not shown) the distribution was not detectably different from the 92 day image. Since the distribution caused by centrifuging is along the drainage capillary pressure curve and the reequilibration is along the imbibition capillary pressure curve one would not expect a uniform distribution to be reached if there is significant hysteresis. There was a small break in the saturation at the low end in Fig. 10C and 10D. This suggests an area with different properties than the rest of the core allowing this area to reach about 2/3rds the saturation of the core immediately above and below it. Perhaps this is a higher permeability zone which would show lower hysteresis.

Previous experiments with centrifuged brine (Baldwin and Yamanashi, 1988b) showed that brine redistributed more slowly than heptadecane. Thus, freezing was not necessary for the brine in Berea Sandstone and chalk, Fig. 11 and 12, respectively. The pressure at the top of the plug was 1.9 psi for Berea Sandstone and 64 psi for the chalk. The saturation gradient produced by centrifuging, although significant, was not as sharp as with the heptadecane. This is probably due to the higher interfacial tension for the brine, about 75

dynes/cm, than for the heptadecane, about 20 dynes/cm for pure hydrocarbons. In both core types no movement of the brine was detected over a 19 day period. At longer times some change in the saturation at the lower end, highest saturation, was noted, however, this appeared to be evaporation rather than redistribution by capillary forces. The lack of achieving a uniform distribution of brine in a short time period has the potential for serious consequences during electrical measurements on cores desaturated by centrifuging. On a more optimistic note, for core centrifuged at higher pressure, Fig. 13, the saturation gradient is small, to not detectable, and therefore should not have as much effect as in those plugs centrifuged at lower pressures.

The images in Fig. 13 demonstrate that even under relatively mild conditions, about 8 psi, the Hassler condition of 100 % saturation at the bottom of the centrifuged plug was not achieved. Even with a resolution of 1.2 mm/pixel a 100 % saturated layer 300 um thick would double the intensity of the pixels across the bottom of the plug, left-hand edge of the image in Fig. 13B.

Fig. 14 shows the effect of water flooding a water-wet core which had been driven to residual hydrocarbon saturation by centrifuging. This relates to possible additional release of oil and ultimately production of tightly bound oil through EOR processes. The core was first saturated with heptadecane and then centrifuged at a high speed, 95 psi at the top, to a residual hydrocarbon saturation. The fully saturated core was easily imaged (Fig. 14A) while at 22% heptadecane saturation no image was obtained (Fig. 14B). The lack of image indicates that the heptadecane was strongly adsorbed to the surface or located in small pores, both of which would give shorter relaxation times than could be imaged at an echo time of 26 ms. Note again that there is no indication of 100% saturation at the bottom of the centrifuged plug. After being immersed in doped brine for 2 days the image in Fig. 14C was obtained. The dopant,  $MnCl_2$ , reduces the brine relaxation time so that it was not detected in Fig. 14C. The intensity, all from the displaced residual hydrocarbon, was 25% of the original intensity. This implies that the water quantitatively displaced the heptadecane from the surface and small pores and relocated it in the large pores where it had a relaxation time, and intensity per molecule, similar to the original heptadecane in the large pores. The lower intensity in Fig. 14C was due to a smaller number of molecules left in the core rather than interaction with the surface or trapping in small pores, as observed in Fig. 14B. In contrast to the centrifuged cores all movement due to water flooding appeared to be complete within 48 hrs. The probable cause for this difference in apparent rate of movement is the distance the heptadecane had to move to be relocated from a surface or small pore into a larger pore is on the order of the pore dimensions. The relatively uniform distribution of the heptadecane in the flooded image suggested no mass migration.

The images, and lack thereof, in Fig. 15 show the results of local environment on the ability to image core. At an echo time of 26 ms no image was obtained from a shaly sandstone, Fig. 15A, even though this core had 20% porosity filled with brine. The images should be rectangles centered in the circles of Fig. 15A. On a research NMR Imager, which could achieve an echo time of 2 ms, the core plug was readily imaged, Fig. 15B. In this case the plug was imaged across the plug producing the circular images. The bright rind around the

plug was free water trapped between the plastic bag and the core. This ability to image only at short echo times indicates that the relaxation time must be very short. Reasons for short relaxation times include the presence of ferromagnetic or paramagnetic species, a strong molecular interaction or small pores. Fig. 16 shows SEM micrographs at two magnifications of pores in this plug. The chlorite clay provides a network of small pores which could be responsible for this short relaxation time. This interpretation is consistent with the bound water which may affect resistivity measurements (Timur, 1969; Givens, 1987). In addition, this core was found to contain magnetite.

### CONCLUSION

NMR Imaging, using a medical instrument, can provide information about cores which cannot be determined by conventional core analysis. Variations in the distribution of pores were on a mm scale for Berea Sandstone and less than mm scale in chalk. Non-uniform saturation distribution was readily detected. Internal structure of the pore network, which could significantly affect further core analysis, was detected with no effect on the core. Saturation gradients in centrifuged core were quantitatively determined. Redistribution of wetting fluids in centrifuged cores was much slower than anticipated, some have not returned to a uniform saturation in a year. Displacement of a residual hydrocarbon by water in a water-wet core was rapid and quantitative. The intensity of the image was shown to be affected by local conditions. These examples merely indicate the potential of NMR Imaging for use in core analysis.

### ACKNOWLEDGMENT

The authors wish to express their appreciation to P. C. Hagen and T. L. Nichols (Phillips Petroleum Co.) for their help in sample preparation.

### REFERENCES

- Baldwin, B. A. and Yamanashi, W. S., 1988a, "NMR Imaging of Fluid Dynamics in Reservoir Core" *Magnetic Resonance Imaging*, Vol. 6, pp. 493-500.
- Baldwin, B. A. and Yamanashi, W. S., 1988b, "Persistence of Non-Uniform Brine Saturation Distribution in SCA Electrical Resistivity Study Core Plugs after Desaturation by Centrifuging," *The Log Analyst*, accepted for publication.
- Bottomley, P. A., Hardy, C. J., Argersinger, R. E. and Allen-Moore, G., 1987, "A Review of <sup>1</sup>H Nuclear Magnetic Resonance Relaxation in Pathology: Are T1 and T2 Diagnostic?" *Med. Phys.* Vol. 14, pp. 1-37.
- Givens, W. W., 1987, "A Conductive Rock Matrix Model (CRRM) for the Analysis of Low-Contrast Resistivity Formations," *The Log Analyst*, Vol. 28, pp. 138-51.
- Hunt, P. K., Engler, P. and Bajsarowicz, C., 1988, "Computed Tomography as a Core Analysis Tool: Applications, Instrument Evaluation, and Image Improvement Techniques," *J. Petro. Tech.*, Vol. 40, pp. 1203-10.
- Lauffer, D. E., 1981, Method for Determining Pore Size Distribution and Fluid Distribution in Porous Media, US Patent # 4,291,271.

Rothwell, W.P. and Vinegar, H. J., 1985, Petrophysical Applications of NMR Imaging Applied Optics, Vol. 24, pp. 3969-72.

Timur, A., 1969, "Pulsed Nuclear Magnetic Resonance Studies of Porosity, Movable Fluid, and Permeability of Sandstones," J. Petro. Tech., Vol. 21, pp. 775-86.

Wellington, S. L., and Vinegar, H.J., 1987, "X-Ray Computerized Tomography," J. Petro. Tech., Vol. 39, pp. 885-898.

### Table of Figures

- 1) NMR receiving coil and holder
- 2) Central NMR Image of fluid saturated Berea Sandstone plug
- 3) NMR intensity profile along the line shown in Fig. 2
- 4) Central NMR Image of fluid saturated chalk with a partially saturated central portion
- 5) Comparison of NMR Images of an intact plug and photographs of the same plug slabbed along the image planes; A - NMRI #3, B - Photograph #3, C - NMRI #4, D - Photograph #4
- 6) Normalized fluid distribution in a composite Berea Sandstone plug; Cross - NMR intensity, Square - Gravimetric
- 7) Calibration curve to convert NMR intensity to saturation for heptadecane in Berea Sandstone
- 8) Fluid saturation distribution using the calibration curve in Fig. 7 to convert the NMR intensity in Fig. 6 to saturation; Cross - NMRI saturation, Square - gravimetric saturation
- 9) Heptadecane distribution in Berea Sandstone as a function of time after centrifuging; A - 0.25 hrs, B - 8 hrs, C - 47 hrs, D - 96 hrs
- 10) Heptadecane distribution in chalk as a function of time after centrifuging; A - 2 hrs, B - 40 days, C - 56 days, D - 92 days
- 11) Brine distribution in Berea Sandstone as a function of time after centrifuging; A - .25 hrs, B - 4 days, C - 14 days, D - 19 days
- 12) Brine distribution in chalk as a function of time after centrifuging; A - 2 hrs, B - 8 days, C - 14 days, D - 19 days
- 13) Brine distribution in Berea Sandstone after centrifuging at high pressure; A - 8.2 psi max, B - 90.5 psi max
- 14) Expulsion of residual hydrocarbon by water from a water-wet Berea Sandstone core; A - Heptadecane Saturated, B - Residual Heptadecane, C - Displaced Heptadecane
- 15) Attempts to obtain images at two echo times; A - 26 ms, B - 2 ms
- 16) Clay on surface of core which could not be imaged at 26 ms echo time



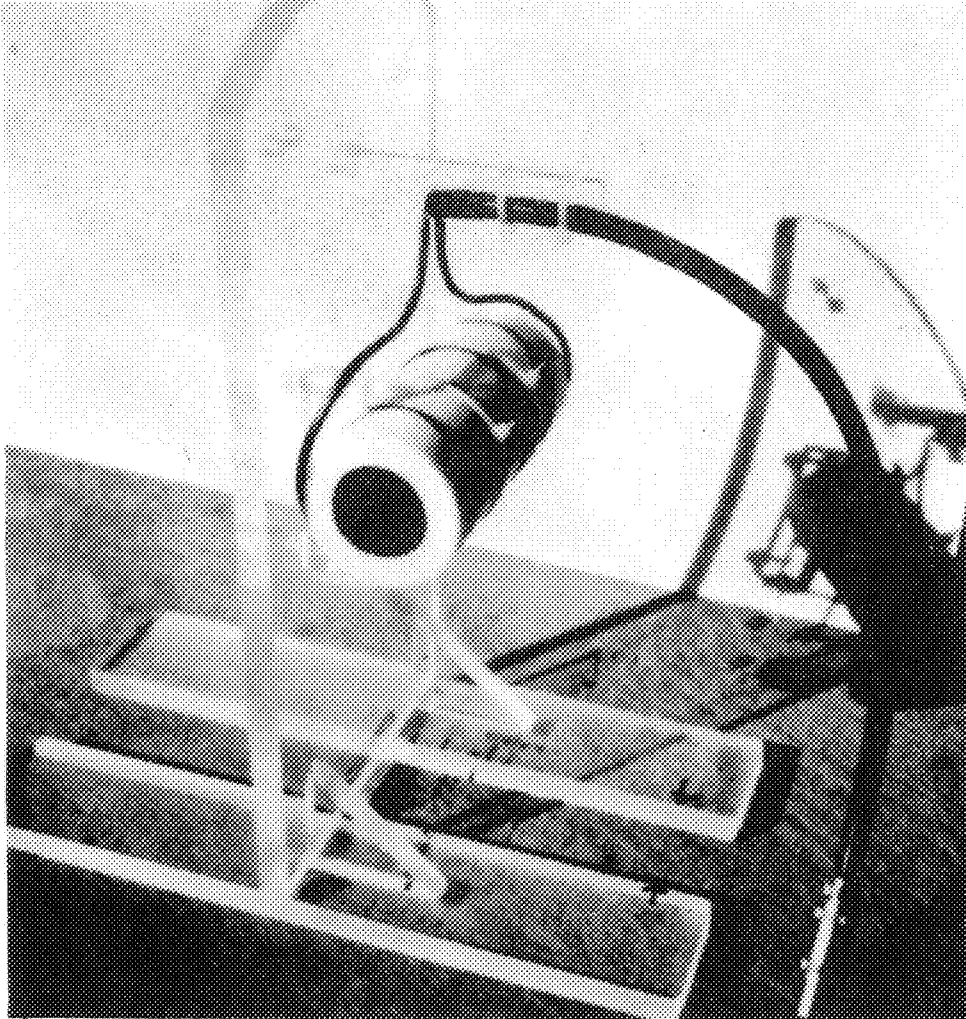


Fig. 1 NMR receiving coil and holder

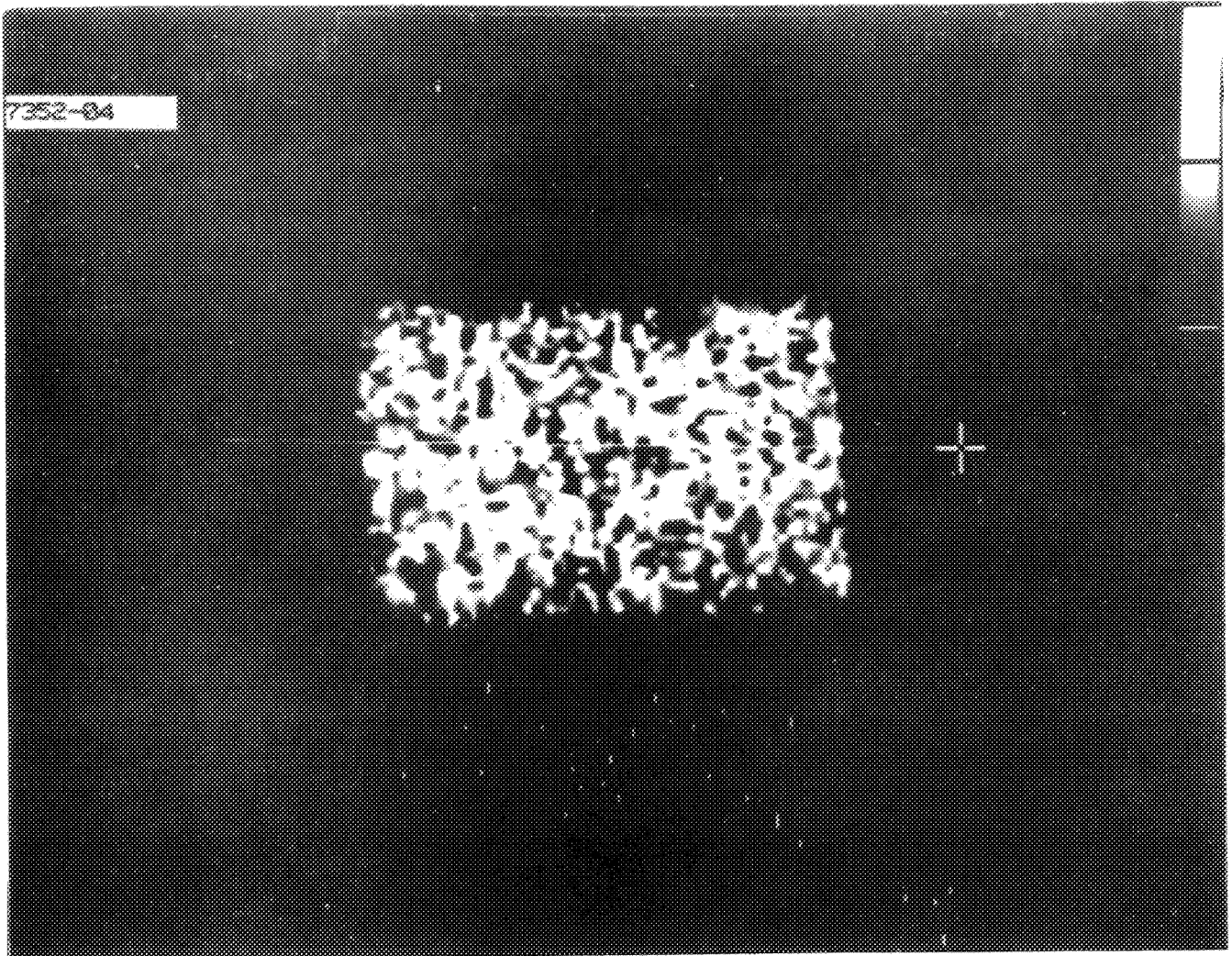


Fig. 2 Central NMR image of fluid saturated Berea Sandstone plug

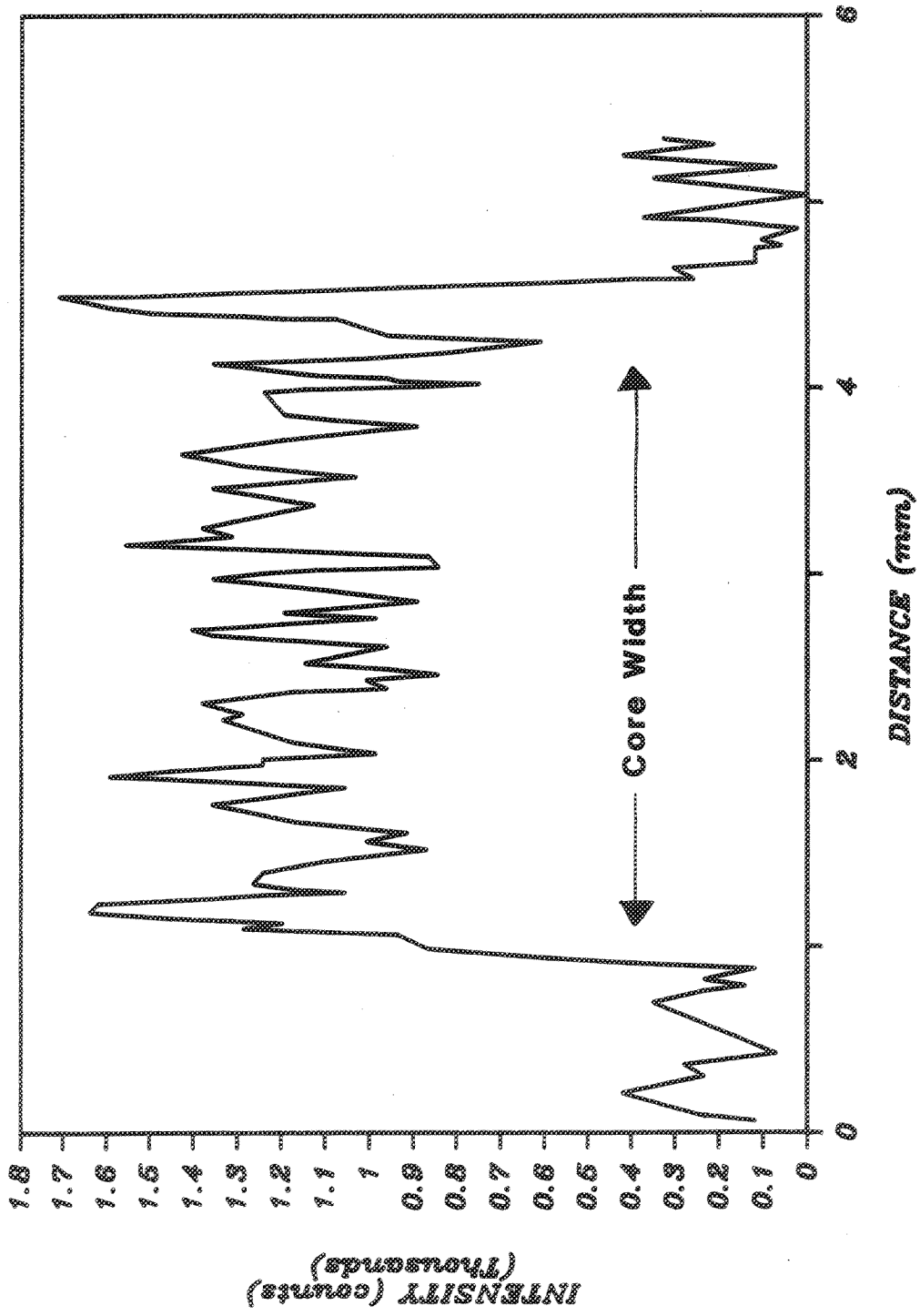


Fig. 3 NMR intensity profile along the line shown in Fig. 2

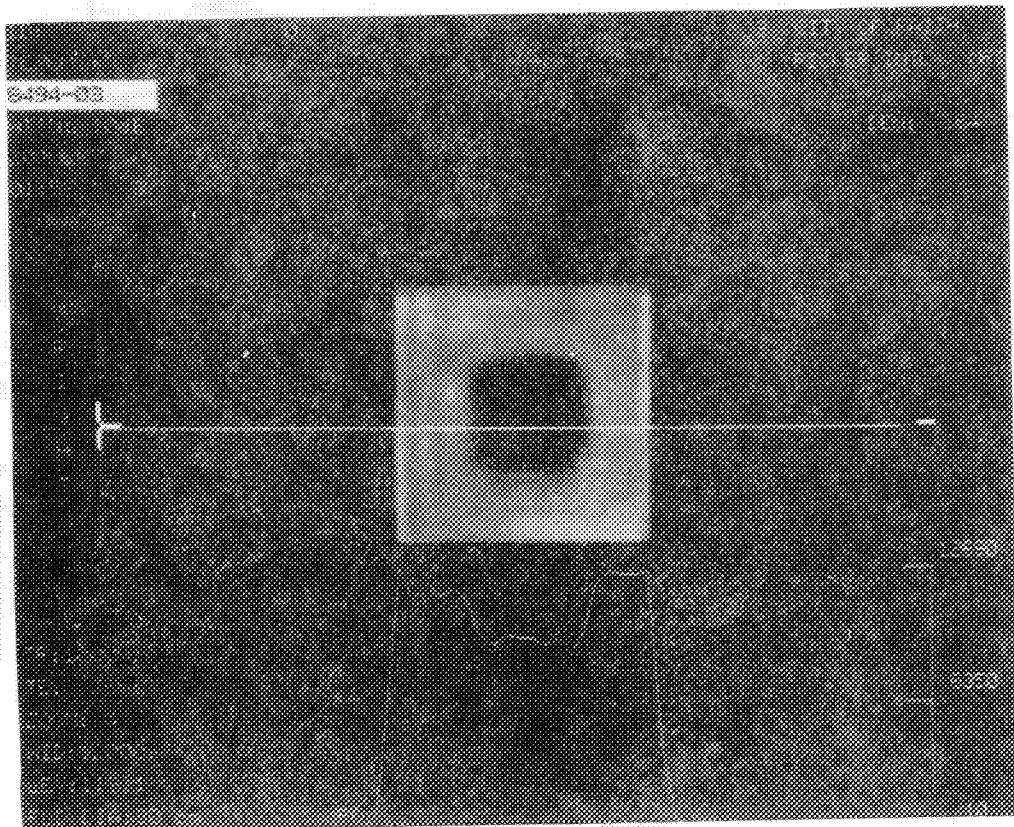
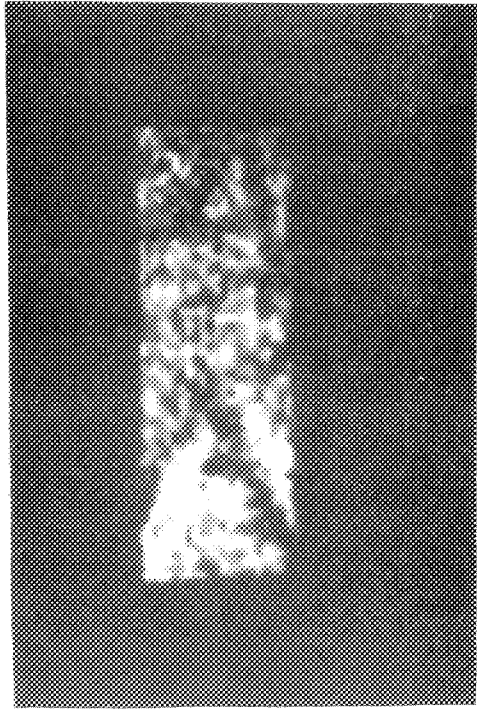
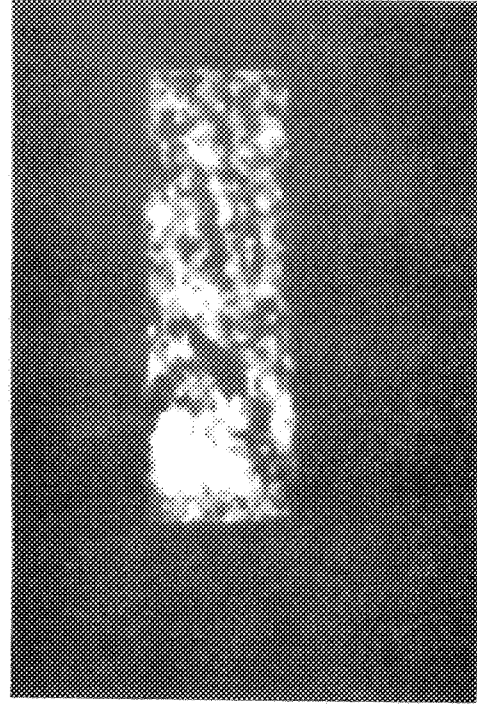


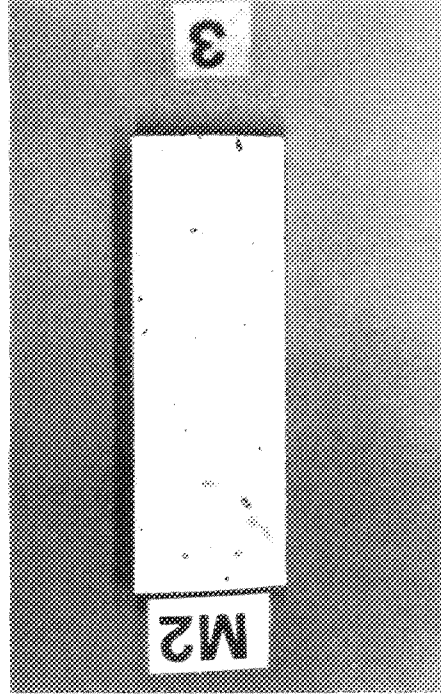
Fig. 4 Central NMR image of fluid saturated chalk with a partially saturated central portion



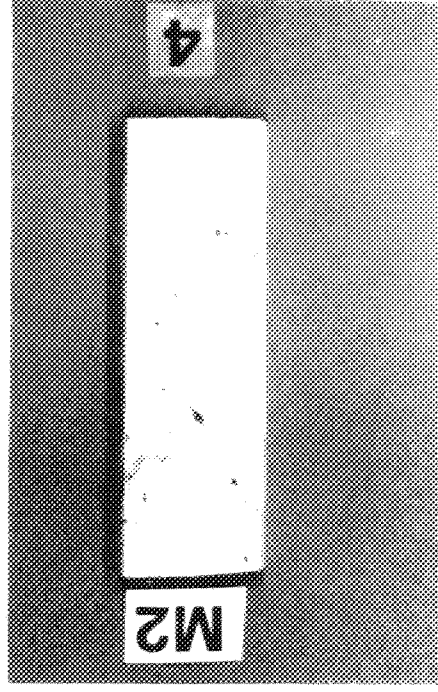
A



C



B



D

Fig. 5 Comparison of NMR images of an intact plug and photographs of the same plug slabbed along the image planes; A - NMR1 //3, B - Photograph //3, C - NMR1 //4, D - Photograph //4

# 1/4 " BEREA SANDSTONE DISCS

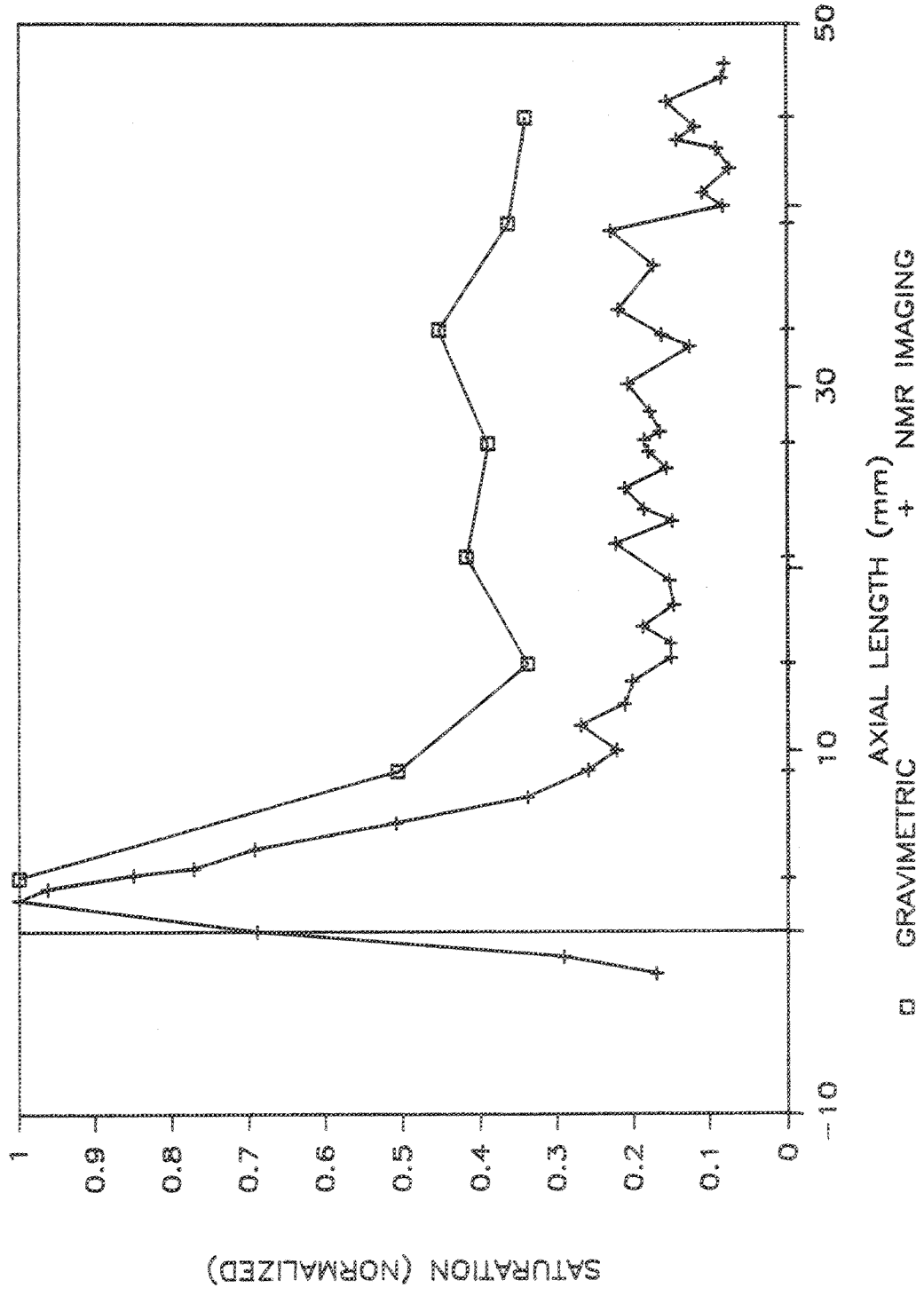


Fig. 6 Normalized fluid distribution in a composite Berea Sandstone

Plug; Cross - NMR intensity, Square - Gravimetric

# MRI CALIBRATION CURVE

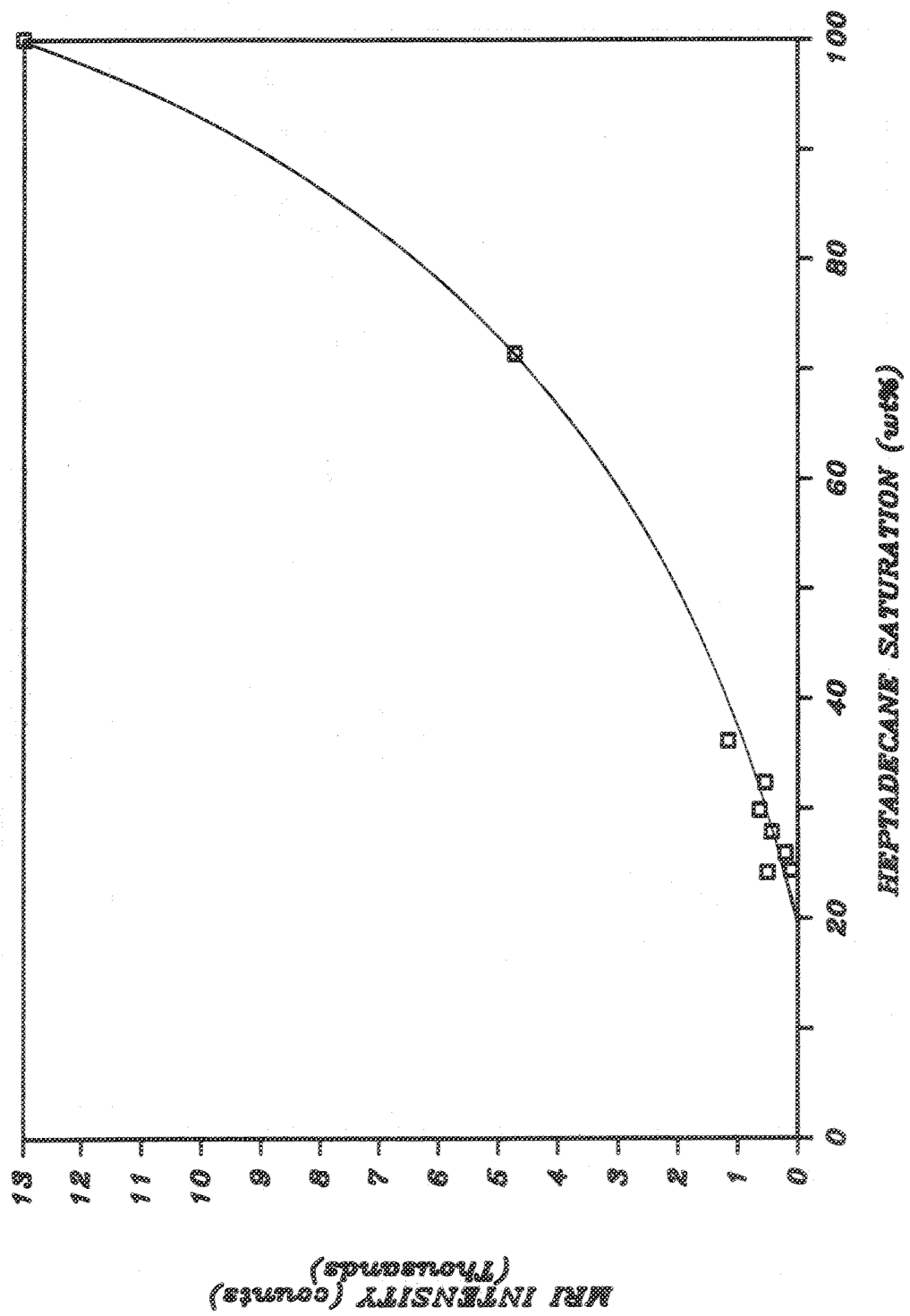


Fig. 7 Calibration curve to convert NMR intensity to saturation for heptadecane in Berea Sandstone

# 1/4 " BEREA SANDSTONE DISCS

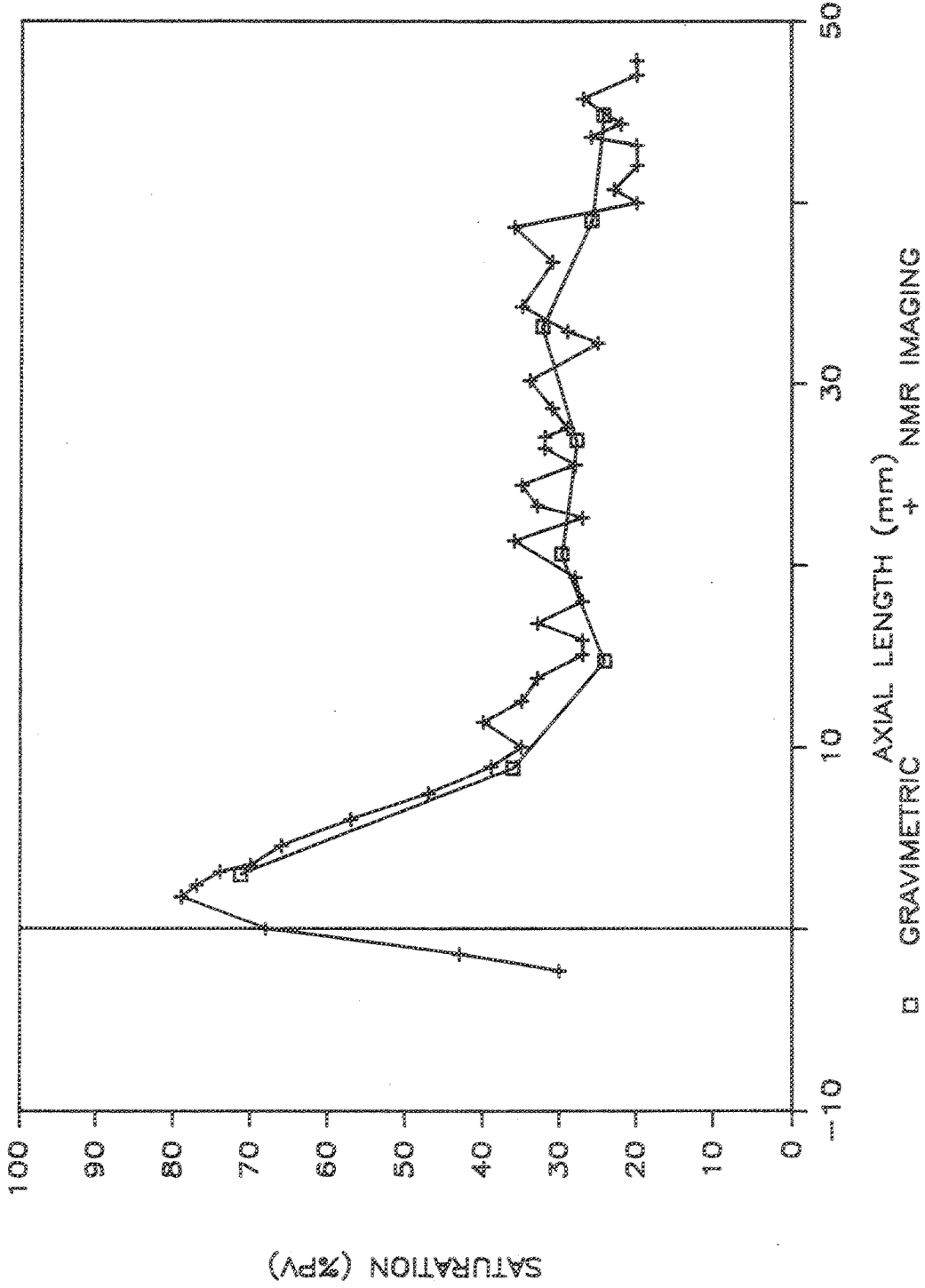
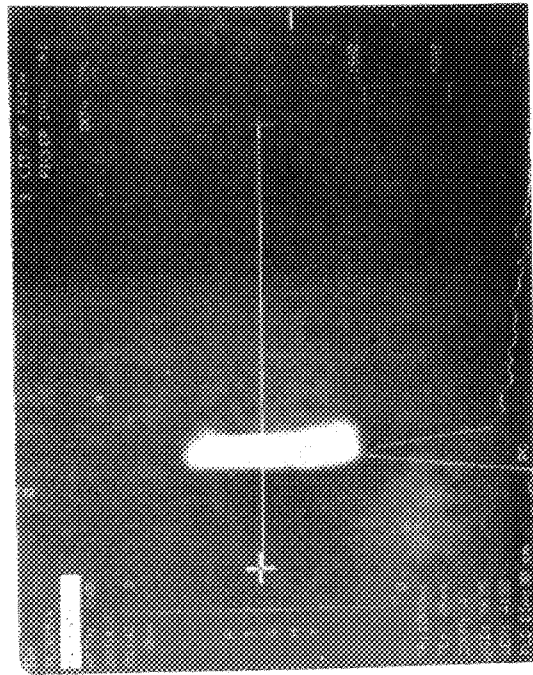
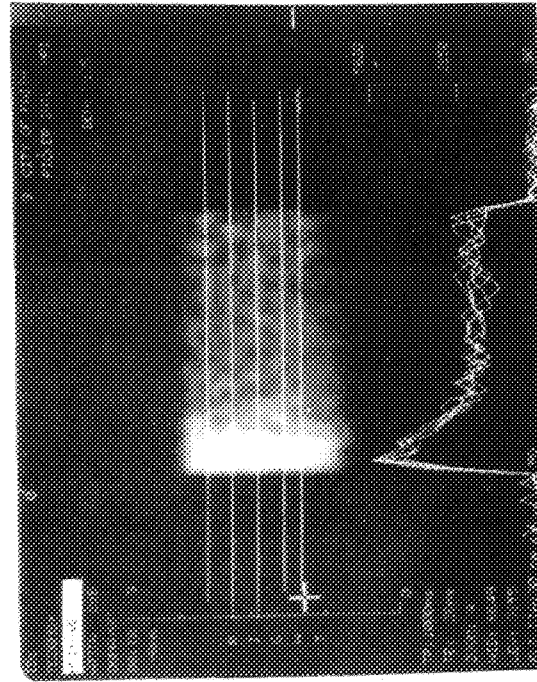


Fig. 8 Fluid saturation distribution using the calibration curve in Fig. 7 to convert the NMR intensity in Fig. 6 to saturation; Cross - NMR saturation, Square - Gravimetric saturation

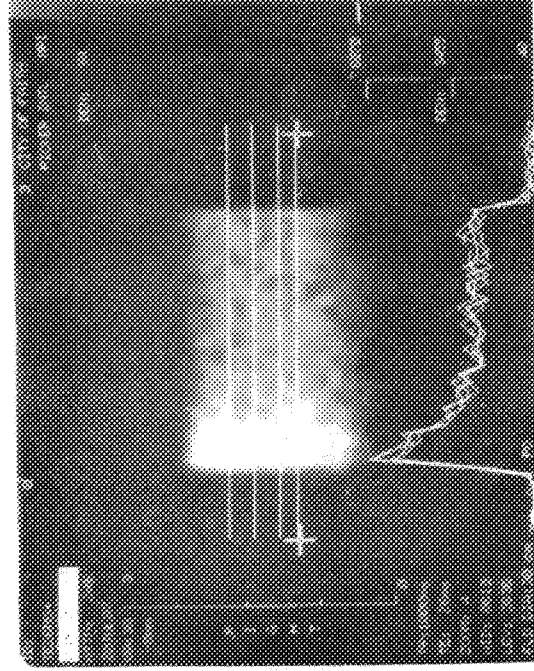




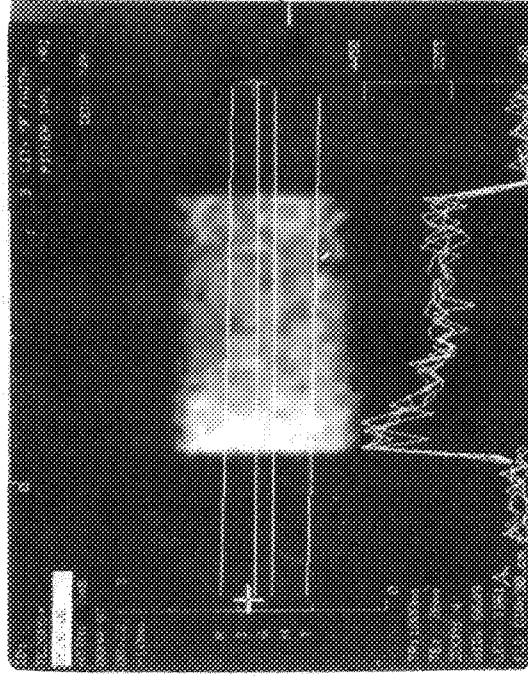
A



C



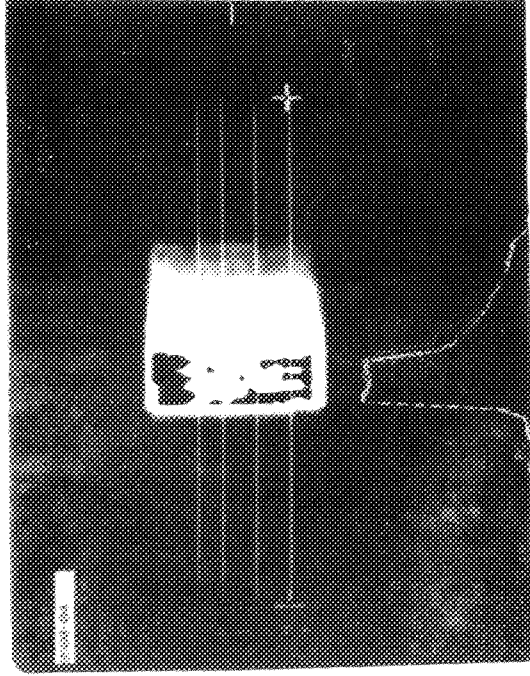
B



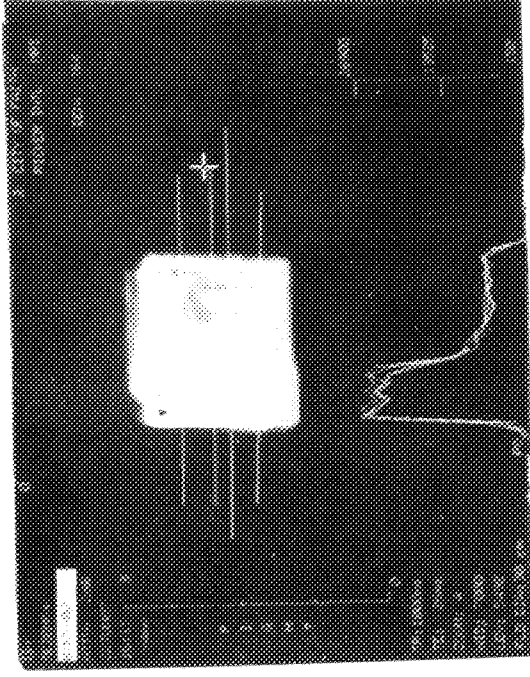
D

Fig. 9 Heptadecane distribution in Berea Sandstone as a function of time after centrifuging:

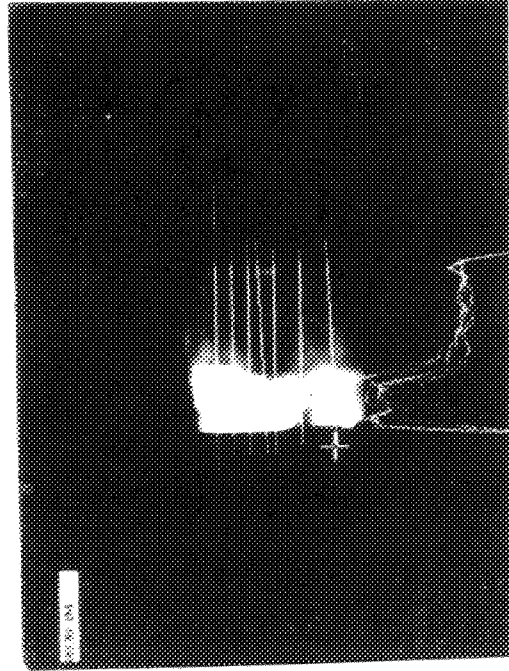
A - 0.25 hrs, B - 8 hrs, C - 47 hrs, D - 96 hrs



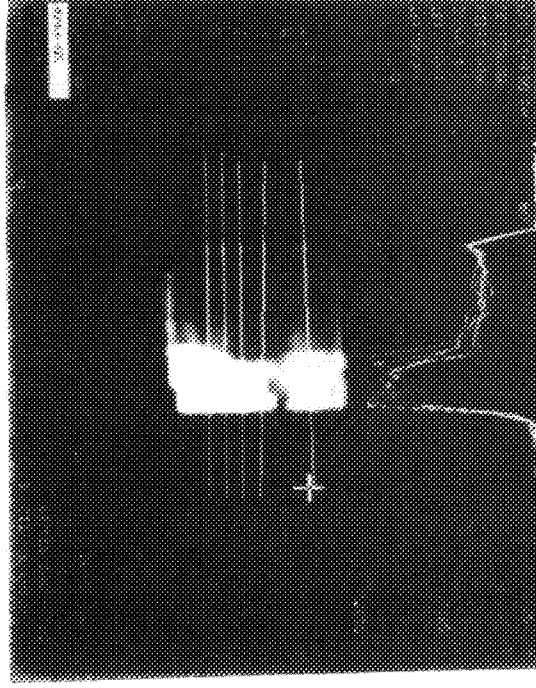
A



B



C



D

Fig. 10 Heptadecane distribution in chalk as a function of time after centrifuging;

A - 2 hrs, B - 40 days, C - 56 days, D - 92 days

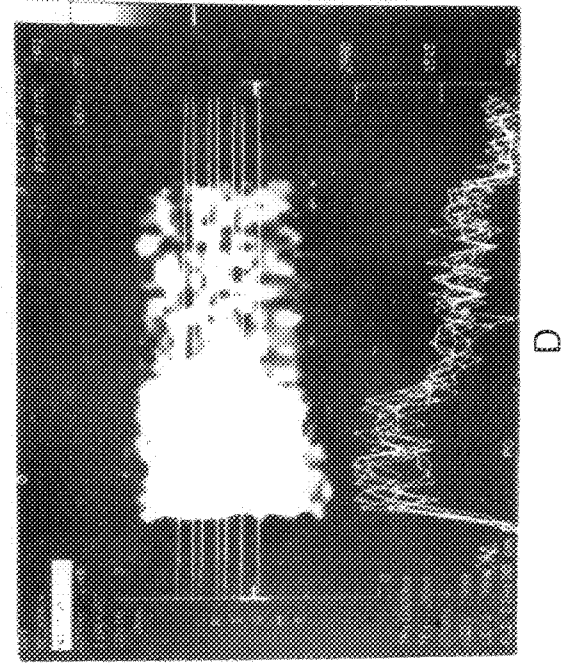
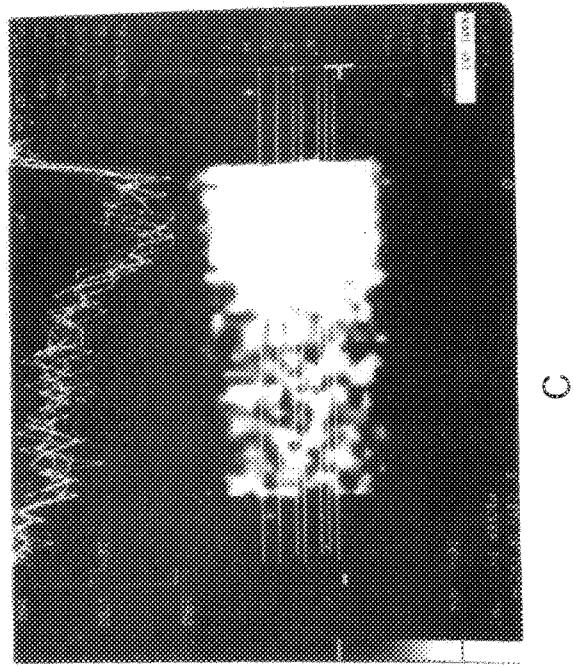
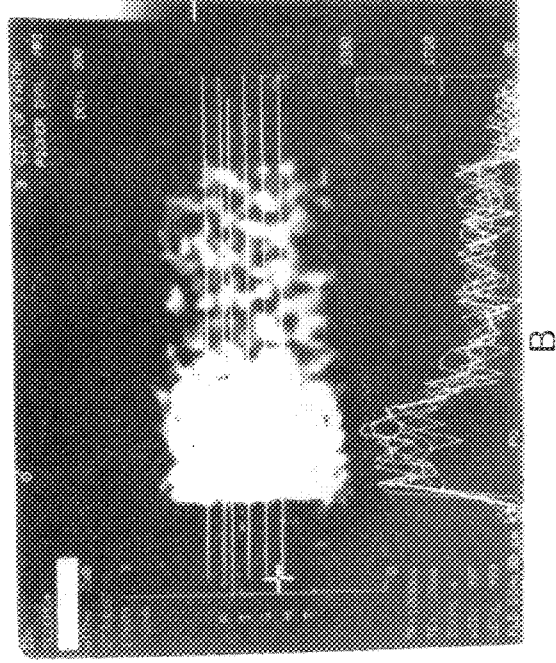
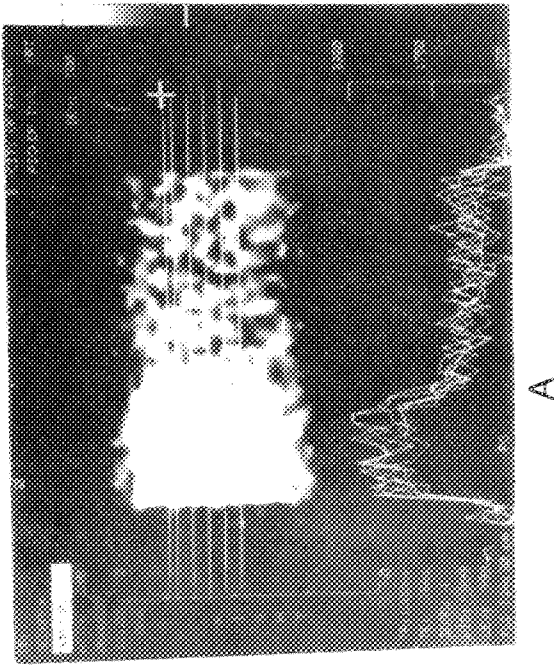
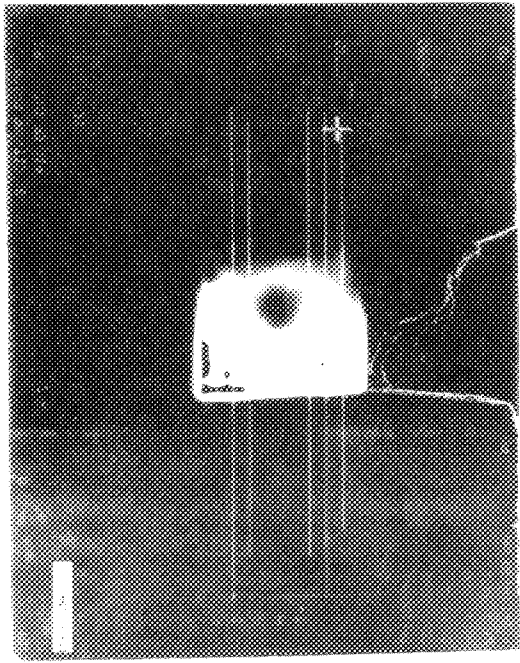
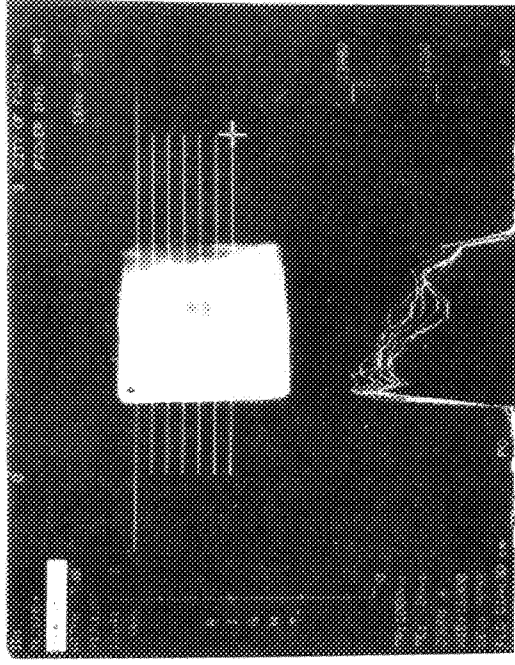


Fig. 11 Brine distribution in Berea Sandstone as a function of time after centrifuging:

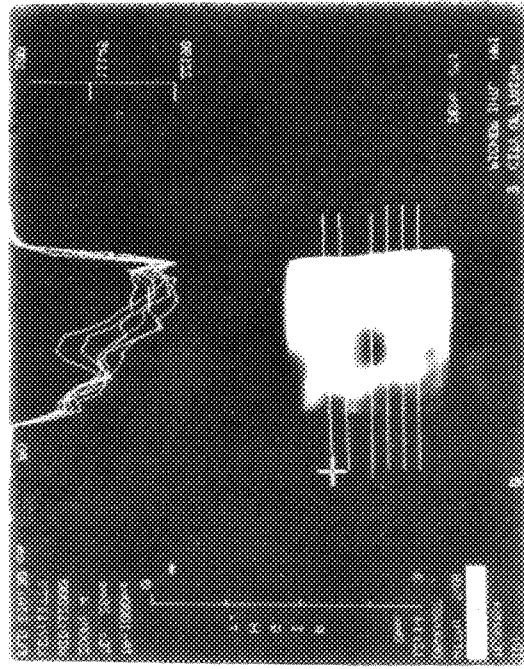
A - 0.25 hrs, B - 4 days, C - 14 days, D - 19 days



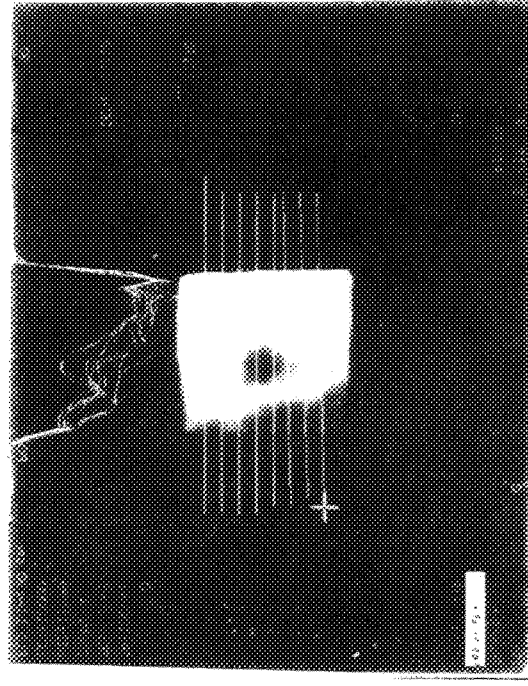
A



B



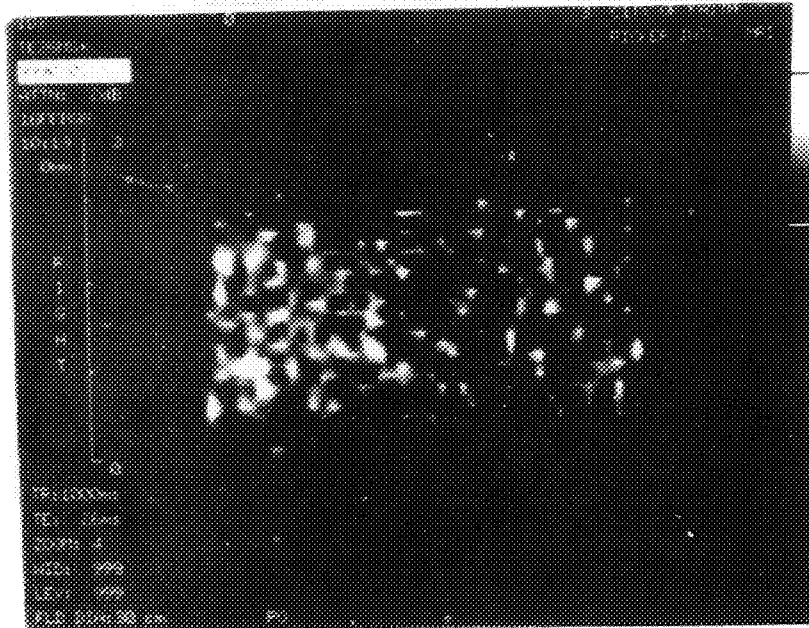
C



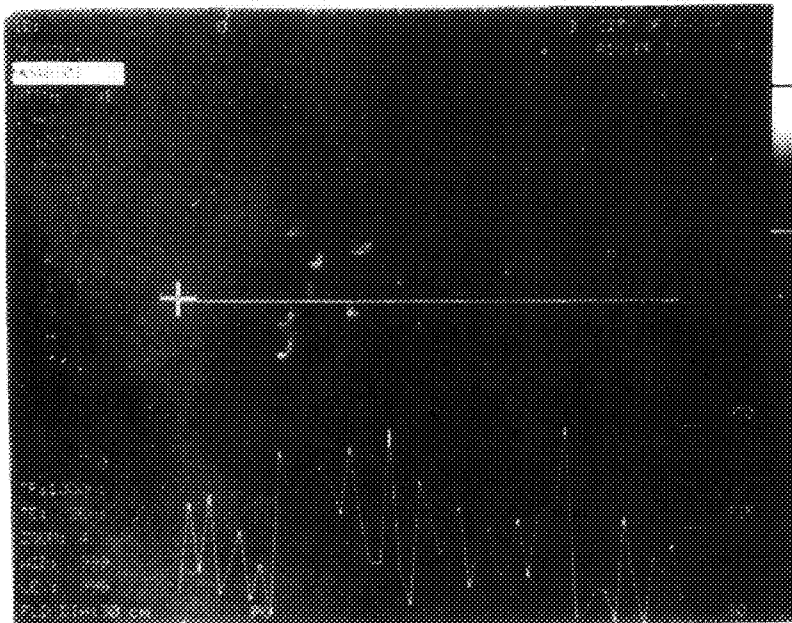
D

Fig. 12 Brine distribution in chalk as a function of time after centrifuging;

A - 2 hrs, B - 8 days, C - 14 days, D - 19 days

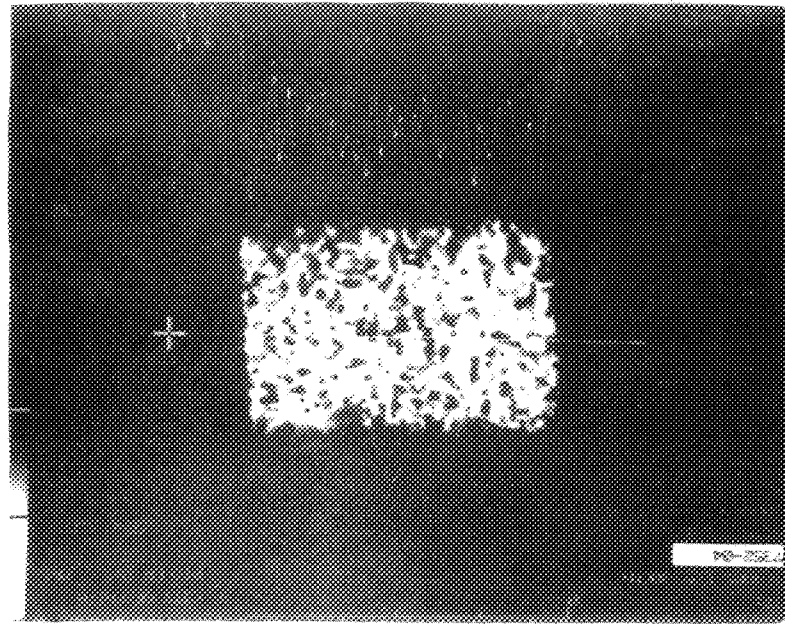


A

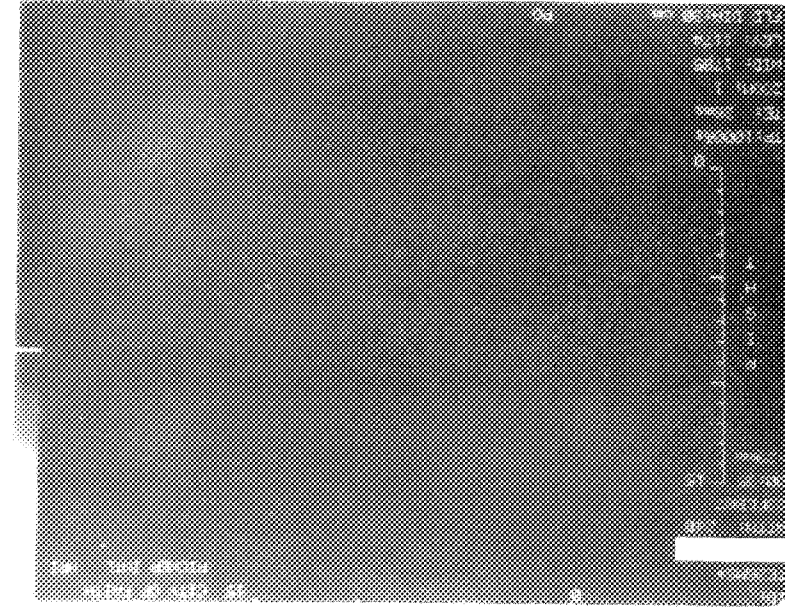


B

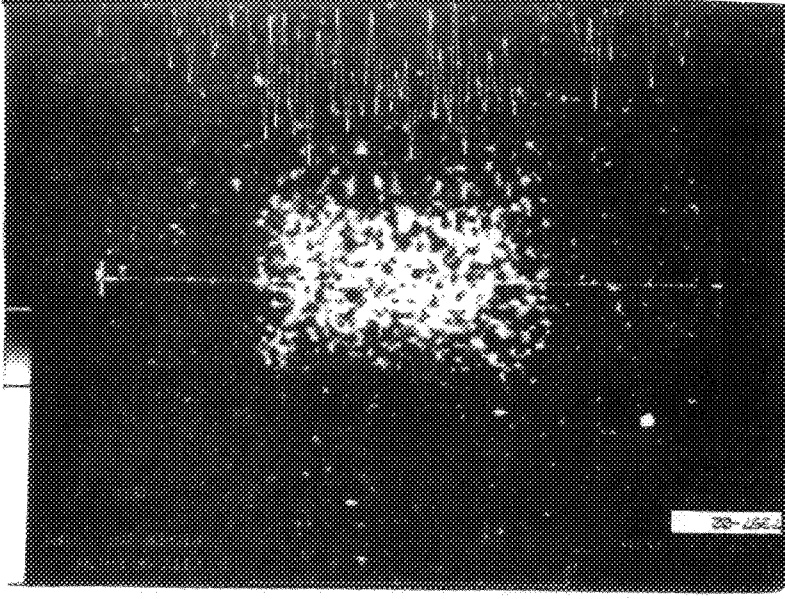
Fig. 13 Brine distribution in Berea Sandstone after centrifuging at high pressure ; A - 8.2 psi max, B - 90.5 psi max



A



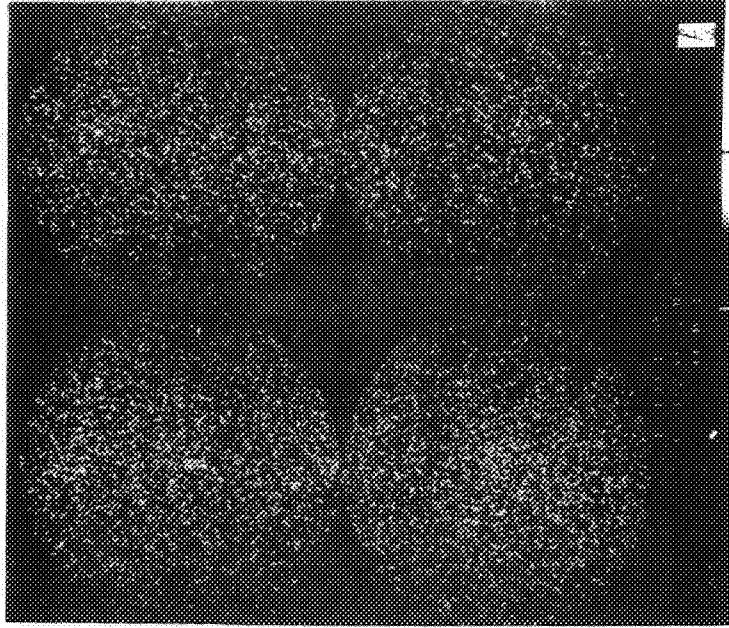
B



C

Fig. 14 Expulsion of residual hydrocarbon by water from a water-wet Berea Sandstone plug;

A - Heptadecane saturated, B - Residual Heptadecane, C - Displaced Heptadecane



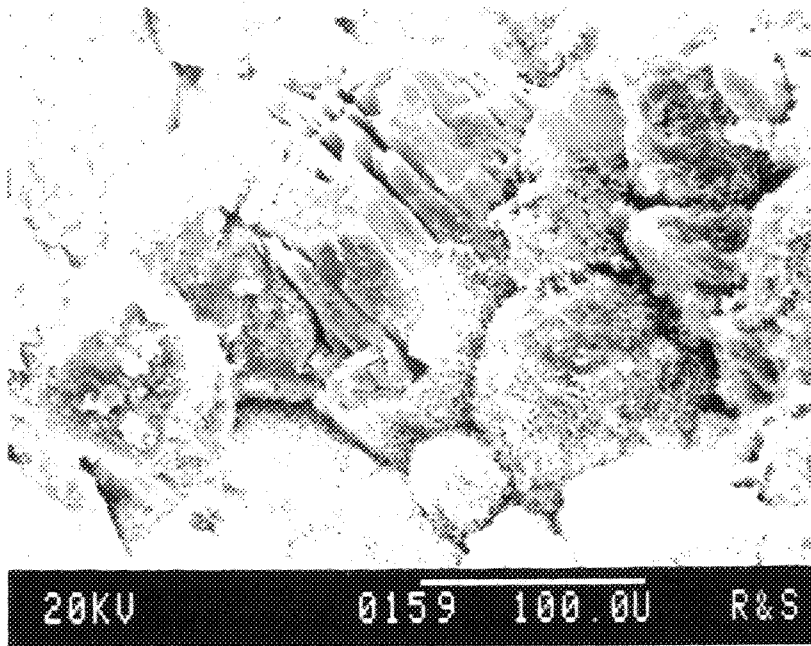
A



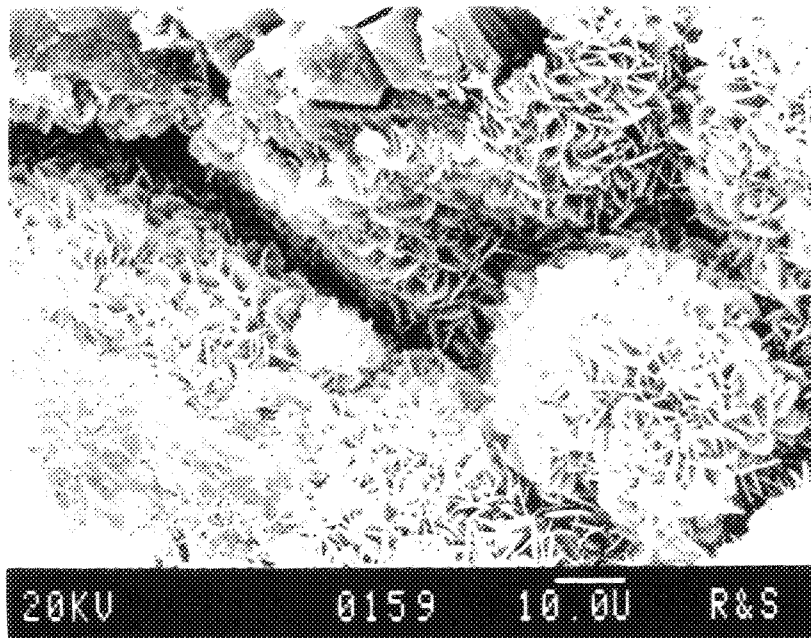
B

Fig. 15 Attempts to obtain images at two echo times:

A - 26 ms, B - 2 ms



A



B

Fig. 16 Clay on surface of core which could not be imaged at 26 ms echo time



# **VIII**

**Preprints for the SCA  
Annual Technical Conference  
Houston, Texas-1988**

